3538 *Inorg. Chem.* **1994**, *33*, 3538–3543

A Density Functional Study of the MLCT States of $[Ru(bpy)_3]^{2+}$ in D_3 Symmetry

Claude Daul*

Institut de Chimie Inorganique et Analytique, CH 1700-Fribourg, Switzerland

Evert J. Baerends and Pieter Vernooijs

Free University of Amsterdam, NL 1081 HV-Amsterdam, The Netherlands

Received April 15, 1993⊗

A density functional based first principles study of the metal to ligand charge-transfer (MLCT) states of $[Ru(bpy)_3]^{2+}$ is presented. The method used in this study includes first-order electrostatic multiplet splitting as well as spin–orbit interaction. The results obtained show that there is an important mixing of the excited singlet and triplet states. These first principles results are in good overall agreement with the observed absorption spectra, with respect to both the spread of the excitation energies and the positions of the strong, unambiguously assigned peaks. Our calculation finds the lowest excited states to be virtually degenerate A_1 and E spin–orbit components of the $(d\pi{:}a_1) \rightarrow (\pi^*{:}a_2)\ {}^3A_2$ state, the former lying a few 10-cm^{-1} units below the latter one. The next excited triplet, i.e. $(d\pi{:}e) \rightarrow (\pi^*{:}a_2)\ {}^3E$, arises only roughly 1500 cm^{-1} above the ${}^3A_2$.

1. Introduction

The electronic structure of $[Ru(bpy)_3]^{2+}$ (bpy = 2,2′-bipyridine) has been investigated for nearly two decades, but the assignment of the lowest excited states remains contradictory.[1-5] Many results were explained by a localized model for these excited states, placing the electron on a single bpy ligand.[2,4,6,7] On the other hand from the results of investigations of single crystals, it was possible to deduce that the lowest two excited states of the $[Ru(bpy)_3]^{2+}$ chromophore are of degenerate E character in the relevant point group D_3.[8-12] Despite their importance, an accurate quantum-mechanical description of the electronic fine structure of the MLCT excited states has not yet been undertaken. In particular, no prediction of the energetical ordering of the MLCT states based on first principle calculation is available. The reason for this is twofold: (i) The first principle calculation of Hartree–Fock (+CI) or density functional (DF) type of excited states of such a large molecule is not straightforward and (ii) the multiplet structure is rather complex. As much as 6 A_1, 6 A_2, and 12 E components are expected within the MLCT manifold, some of them being only separated by a few wavenumbers.

Nevertheless we have recently demonstrated that such calculations are feasible,[13,14] and even though the experimental spacing between two excited states (a few cm^{-1}) is far below the accuracy (several hundred cm^{-1}) of our method, we do believe that such a calculation is useful to the scientific community. Indeed, the result of such a calculation may be an important aid to spectroscopists for band assignments and for the elaboration of refined models.

In the present communication an electronic structural model that includes both DF calculation of the electrostatic MLCT states and spin–orbit coupling is presented. Several workers, including ourselves, have attempted in the past with varying results to describe the MLCT bands of the title compound.[15-19] Among those, there are only 2 communications which do include an extensive fine-structure calculation of the excited MLCT states. The first one is due to Kober and Meyer[15a] and the second one which is very similar to the first one is due to Ferguson and Herren.[15b] But the models used by those two groups of authors is quite approximate; e.g. the singlet–triplet splitting is described by one single parameter and does not include any calculated energies. The model we present here is different in this respect since only the value of the spin–orbit coupling constant of Ru is not calculated from first principles.

2. Computational Methods

2.1 Density Functional Calculations. The density functional calculations reported in this paper have been carried out with the Amsterdam density functional (ADF) program package.[20-22] The computational scheme is characterized by a density fitting procedure to obtain the Coulomb potential[20] and by elaborate 3D numerical integration techniques[21,22] for the evaluation of the Hamiltonian matrix elements, including those of the exchange-correlation potential. The Vosko–Wilk–Nusair parameterization[23] of the electron gas data has been used for the exchange-correlation energy and potential. The molecular orbitals were expanded in an uncontracted double-ζ STO basis set for the C, N, and H atoms,

---

⊗ Abstract published in *Advance ACS Abstracts*, June 15, 1994.

(1) Harrigan, R. W.; Crosby, G. A. *J. Chem. Phys.* **1973**, *59*, 3468. Baker, D. C.; Crosby, G. A. *Chem. Phys.* **1974**, *4*, 428.

(2) Kober, E. M.; Meyer, T. J. *Inorg. Chem.* **1984**, *23*, 3877.

(3) Krausz, E. *Chem. Phys. Lett.* **1987**, *135*, 429.

(4) Myrick, M. L.; Blakley, R. L.; DeArmond, M. K.; Arthur, M. L. *J. Am. Chem. Soc.* **1988**, *110*, 1325.

(5) Krausz, E.; Ferguson, J. *Prog. Inorg. Chem.* **1989**, *37*, 293.

(6) Bradley, P. G.; Kress, N.; Hornberger, B. A.; Dallinger, R. F.; Woodruff, W. H. *J. Am. Chem. Soc.* **1981**, *103*, 7441.

(7) Riesen, H.; Krausz, E., Puza, M. *Chem. Phys. Lett.* **1988**, *151*, 65. Riesen, H.; Krausz, E. *Chem. Phys. Lett.* **1988**, *151*, 71.

(8) Yersin, H.; Gallhuber, E. *J. Am. Chem. Soc.* **1984**, *106*, 6582.

(9) Yersin, H.; Gallhuber, E.; Hensler, G. *J. Phys. (Paris)*, **1985**, *46C7*, 453.

(10) Yersin, H.; Gallhuber, E.; Hensler, G.; Schweitzer, D. *Chem. Phys. Lett.* **1989**, *161*, 315.

(11) Yersin, H.; Braun, D.; Hensler, G.; Gallhuber, E. In *Vibronic Processes in Inorganic Chemistry*; Flint, C. D., Ed.; Kluwer: Dordrecht, The Netherlands, 1989; p 195.

(12) Braun, D.; Gallhuber, E.; Yersin, H. *Chem. Phys. Lett.* **1990**, *171*, 122. Yersin, H.; Braun, D. *Coord. Chem. Rev.* **1991**, *111*, 39.

(13) Bellafrouh, K.; Daul, C. *Proceedings of the 4th International Conference on the Application of Density Functional Theory in Chemistry and Physics*; Ascona, Switzerland, 1991.

(14) Daul, C.; Güdel, H. U.; Weber, J. *J. Chem. Phys.* **1993**, *98*, 4023.

(15) (a) Kober, E. M.; Meyer, T. J. *Inorg. Chem.* **1981**, *21*, 3967. (b) Ferguson, J.; Herren, F. *Chem. Phys.* **1983**, *76*, 45.

(16) Ceulemans, A.; Vanquickenborne, L. G. *J. Am. Chem. Soc.*, **1981**, *103*, 2238.

(17) Daul, C.; Weber, J. *J. Chem. Phys. Lett.* **1981**, *79*, 593.

(18) Belser, P.; Daul, C.; Zelewsky, A. v. *Chem. Phys. Letters* **1981**, *79*, 596.

(19) Mayoh, B.; Day, P. *Theor. Chim. Acta* **1978**, *49*, 259.

(20) Baerends, E. J.; Ellis, D. E.; Ros, P. *Chem. Phys. 2* **1993**, 42.

(21) Boerrigter, P. M.; te Velde, G.; Baerends, E. J. *Int. J. Quantum Chem.* **1988**, *33*, 87.

(22) te Velde, G.; Baerends, E. J. *J. Comput. Phys.* **1992**, *99*, 84.

(23) Vosko, S. H.; Wilk, L.; Nusair, M. *Canad. J. Phys.* **1980**, *58*, 1200.

0020-1669/94/1333-3538$04.50/0

with one 2p set added on H. For Ru a triple-ζ 4d and double-ζ 4s, 4p, and 5s basis was used, augmented with one 5p STO. The cores (C, N, 1s; Ru, 1s–3d) have been kept frozen. The implementation allows one to build up the molecule from constituting fragments, which has the advantage that MOs and Mulliken populations (including orbital compositions) may be expressed in terms of a fragment orbital basis. In the present case both the natural bipyridine fragments and the Ru atom have been used as well as, for reasons to be discussed below, the complete $[Ru(bpy)_3]^{2+}$ in a specific self-consistently converged electronic configuration.

The geometry of $[Ru(bpy)_3]^{2+}$ (D_3 symmetry) was taken from the X-ray diffraction study of Rillema, Jones, and Levy.[24] All the calculations, i.e. both on the ground state and the excited states, were carried out with this geometry. This is justified since excitations to MLCT states do not exhibit any structural relaxation.[12]

The calculation of multiplet energies (see next section) requires the energies of excited determinants, e.g. (occupied spin–orbital no. i) → (empty spin–orbital no. j), to be computed. If either of the two orbitals i or j belongs to a degenerate set of E symmetry in the D_3 point group, the excited determinant will yield an electron density that does not have A_1 symmetry in D_3. In order to calculate the DF energy corresponding to that electron density it is necessary to lower the symmetry to a point group in which the E irrep of D_3 splits, so that the electron density of the excited determinant will be A_1 in the lower symmetry. The appropriate point group in our case is C_2. If we use a complete $[Ru(bpy)_3]^{2+}$ molecule calculated in D_3 symmetry as a "fragment" for a calculation in C_2 symmetry, the calculation immediately converges and the eignevectors, expressed in the D_3 MO's as basis functions, do not show any mixing. The identification of the C_2 eigenvectors in terms of D_3 MO's is then readily made, yielding a direct mapping of the excited D_3 determinant on the equivalent C_2 determinant. The calculation of the energy of an (i) → (j) determinant now proceeds through the following steps. Consider e.g. the excitation energy $[(d\pi{:}e\text{-}1)\alpha] \rightarrow [(\pi^*{:}a_2)\alpha]$. First we calculate self-consistently the spin-restricted configuration $(d\pi{:}e)^3(\pi^*{:}a_2)^1$ in D_3 symmetry. Next we make the correspondence between D_3 and C_2 eigenvectors as described above. The energy difference of e.g. $[(d\pi{:}e\text{-}2)^2 (d\pi{:}e\text{-}1)\beta\, (\pi^*{:}a_2)\alpha\}$ with the spin-restricted excited configuration is then obtained in a one-cycle calculation in C_2 symmetry, using the previous D_3 excited configuration as "fragment" and determining the required orbital occupations from the previously obtained correspondence between C_2 and D_3 eigenvectors. In this procedure, which avoids any convergence problem due to close-lying partially occupied orbitals, the relatively large energetic (exchange) effect due to the unpaired spins is taken into account, but the orbital relaxation effects (spin-polarization) in the spin-unrestricted state are neglected. In fact, the effect of relaxation is very small in this extended system. This was checked in a few test calculations where the spin-unrestricted configurations were converged. The energetic effects of the orbital relaxation have been shown to be very small indeed (cf. Table 5, footnote 2).

2.2 Multiplet Structure. The calculation of the multiplet splittings in density functional (DF) theory has been discussed earlier by Ziegler, Rauk, and Baerends.[25] Following their results, it is possible to replace the energy of a single determinant by the corresponding statistical energy as obtained in DF theory. In the case of symmetrical molecules with degenerate orbitals, the individual multiplet states arising from an open-shell configuration can, in general, not be expressed by a single determinant. That is, DF calculations do not yield multiplet energies directly. According to the aforementioned paper,[25] it is possible to write the energy of a multiplet arising from a given configuration as a weighted sum of single-determinantal energies; one may then obtain the first-order multiplet splittings as solution of a system of M linear equations with N unknowns, where $M \geq N$.[26] However, it is possible, by exploiting symmetry to the largest possible extent, to reduce the number of required determinantal energies and thus keep computational effort to a minimum. A system of computer programs working on both mainframe and personal computers has been developed carrying out for any desired point group the required group theoretical manipulations. It should be pointed out at this place that this method will work for any symmetry point group. However, the higher the molecular symmetry is, the larger will be the benefit. At the limit of no symmetry the method will reduce to the calculation of as many excited configuration as there are excited states considered.

The full details of the method will be published elsewhere,[26] and only a short outline of it follows here. The method consists essentially of making maximum use of the relations that exist between the energies of the determinants of a configuration by symmetry. We will expand those symmetry relations using the traditional approach of writing the energy as the expectation value of the exact Hamiltonian for the determinants, i.e. using the familiar energy expressions in terms of J and K integrals. Exactly the same symmetry relations should exist for the determinantal DFT energies. Approximate density functionals may be deficient in this respect. The small deviations do not concern us here, although it should be noted that strictly obeying the symmetry relations is a useful criterion for judging and constructing approximate density functionals. We stress that the following discussion in terms of J and K integrals and reduced electrostatic matrix elements, as well as the corresponding information in the tables, is only meant to make clear the symmetry relations. The actual energies have been obtained with the above mentioned density functionals, and the described method is essentially a symmetry-based generalization of the procedure by Ziegler, Rauk, and Baerends.[25]

Consider the multiplet wave functions

$$\psi_l = |\alpha \Gamma m_\Gamma S m_S\rangle \tag{1}$$

arising from a given configuration α are easily obtained by vector coupling as

$$\psi_l = \sum_\mu C_{l\mu}\phi_\mu \tag{2}$$

where Γ is the label of the irreducible representation of the space part of the wave function, m_Γ refers to its component in case of degeneracy, S is the spin part of the wave function with component m_S in case of spin multiplicity larger than 1, $\phi_\mu = |\chi_1\chi_2\chi_3...|$, is a single-determinantal wave function of spin–orbitals χ_1, χ_2, χ_3, ..., and $C_{l\mu}$ is an orthogonal square matrix of symmetry coefficients. Let us note that DF or Hartree–Fock calculations provide directly the energies associated with ϕ_μ, which may be interpreted as barycenters of the various energies resulting from the states generated by the corresponding configuration. On the other hand, this energy $E(\phi_\mu)$ can also be obtained from Slater's rules for a single determinant as a sum of Coulombic and exchange integrals (ignoring the constant one-electron part for the determinants of a single configuration):

$$\begin{aligned} E(\phi_\mu) = \sum_{i<j}\{ & \int\int \chi_i^*(1)\chi_j^*(2)G_{12}\chi_i(1)\chi_j(2)\,\mathrm{d}V_1\,\mathrm{d}V_2 - \\ & \int\int \chi_i^*(1)\chi_j^*(2)G_{12}\chi_j(1)\chi_i(2)\,\mathrm{d}V_1\,\mathrm{d}V_2\} = \\ & \sum_{i<j}\{(\chi_i\chi_i|\chi_j\chi_j) - (\chi_i\chi_j|\chi_i\chi_j)\} \end{aligned} \tag{3}$$

$$G_{12} = 1/r_{12}$$

Following e.g. Griffith,[27] these two-electron integrals can in turn be expressed in a limited number of reduced electrostatic matrix elements as follows. Using the spherical harmonic addition theorem for expansion of $1/r_{12}$ and symmetry adapting $Y_{lm}(\theta_1,\varphi_1)$ and $Y_{lm}(\theta_2,\varphi_2)$ to the irreducible representations of the point group, one obtains

$$\frac{1}{r_{12}} = \sum_{f\phi}\sum_i g_{i,f\phi}(1)\, g_{i,f\phi}(2) \tag{4}$$

where f and φ denote irreducible representations and components respectively and $g_{i,f\varphi}$ are one-electron functions. The sum over i enumerates the occurrence of irrep f and is in principle infinite since the sum over (l,m) in the expansion of $1/r_{12}$ is, and each irrep f keeps occurring when the sum over (l,m) is continued. Considering a specific two-electron integral

---

[24] Rillema, D. P.; Jones, D. S.; Levy, H. A. *J. Chem. Soc. Chem. Commun.* **1979**, 849.

[25] Ziegler, T.; Rauk, A.; Baerends, E. J. *Theor. Chim. Acta* **1977**, *43*, 261.

[26] Daul, C. *Proceedings of the 5th International Conference on the Application of Density Functional Theory to Chemistry and Physics*; Como, 1993; to be published in a special issue of *Int. J. Quant. Chem.* in 1994.

[27] Griffith, J. S. *The Theory of Transition Metal Ions*; Cambridge University Press: Cambridge, U.K., 1961.

$$\langle a\alpha(1)\, b\beta(2)|G|c\gamma(1)\, d\delta(2)\rangle$$

where a–d denote irreps and α–δ corresponding components, one obtains, by first expanding $1/r_{12}$ as above and next vector coupling the orbitals a and c belonging to electron 1 and the orbitals b and d belonging to electron 2,[28]

$$\langle a\alpha(1)\, b\beta(2)|G|c\gamma(1)\, d\delta(2)\rangle = \sum_{if\phi}\langle a\alpha(1)\,|g^{(1)}_{if\phi}|c\gamma(1)\rangle\langle b\beta(2)|g^{(2)}_{if\phi}|d\delta(2)\rangle = \sum_{f\phi}V\begin{pmatrix} a & c & f \\ \alpha & \gamma & \phi \end{pmatrix}V\begin{pmatrix} b & d & f \\ \beta & \delta & \phi \end{pmatrix}\sum_{i}\langle a\|g_{if}\|c\rangle\langle b\|g_{if}\|d\rangle \quad (5)$$

Here $\langle a\|g_{if}\|c\rangle$ is a one-electron reduced matrix element of the one-electron operator $g_{if\phi}(1)$ with the irreps $a(1)$ and $c(1)$. The coupling coefficients (Griffith's V-coefficients) are the same for all values of i, and so the sum over i on the right-hand side can be considered as a single reduced electrostatic matrix element:

$$R(ac;bd;f) = \sum_{i}\langle a\|g_{if}\|c\rangle\langle b\|g_{if}\|d\rangle \quad (6)$$

The reduced matrix elements R are nonzero only if both the direct products of a and c and of b and d contain f. Moreover if $a = c$ or $b = d$, f is restricted to the symmetrized square. In the case of e.g. an octahedral ligand field, within the d-manifold, there are exactly 10 different R's as pointed out by Griffith in ref 27. The determinantal energies $E(\phi_\mu)$ are related to Coulomb and exchange integrals (cf. eq 3) which are in turn related through eq 5 to the reduced matrix elements R, and as many DF calculations for determinantal energies $E(\phi_\mu)$ are required as there are R matrix elements in order to solve for the R's. The state energies we seek are obtained as

$$\langle\psi_i|G|\psi_j\rangle = \sum_{\mu,\nu}C_{i\mu}C_{j\nu}\langle\phi_\mu|G|\phi_\nu\rangle \quad (7)$$

and may thus be expressed in terms of two-electron integrals, which in turn are expressed in terms of the minimal number of reduced electrostatic matrix elements or, if preferred, in terms of the minimal number of one-determinantal energies $E(\phi_\mu)$.

Unfortunately this procedure does not necessarily yield all R's. In principle the one-determinantal energies only allow one to obtain Coulomb $(ii|jj)$ and exchange $(ij|ij)$ contributions, i.e. first-order electrostatic interactions contributing to the diagonal term (cf. eq 3 for the notation; i and j refer to MO indices). Second-order, off diagonal, contributions depend upon $(ij|kl)$ elements which are neither of Coulomb nor of exchange type and which can therefore not be obtained from the single-determinant energies $E(\phi_\mu)$. Thus, in cases where second-order electrostatic interaction is important, the off-diagonal two-electron integrals have to be calculated explicitly from the SCF wave functions or approximated by appropriate model calculations. The calculation of such interaction matrix elements in DFT may be useful but at present lacks firm theoretical foundation.

As an illustration of this method, let us consider e.g. the ligand field states of the configuration e^2, of an octahedral d^2 complex. The configuration e^2 generates the three states: $^1A_1$, $^3A_2$, ^1E. Our scheme induces the calculation of only two excited single determinantals within the six possible ones. The four remaining single determinants are redundant, and their energies are expressible as linear combinations of the two former ones. In the example considered, two nonredundant single determinants are e.g. $|e_\epsilon^+e_\epsilon^-|$ and $|e_\epsilon^+e_\theta^+|$. Each of them has a different energy and needs a separate DF calculation. The following multiplet splittings are thus obtained:

$$E(^1A_1) = 4/3E(|e_\epsilon^+e_\epsilon^-) - 1/3E(|e_\epsilon^+e_\theta^+|)$$

$$E(^3A_2) = E(|e_\epsilon^+e_\theta^+)$$

$$E(^1E) = 2/3E(|e_\epsilon^+e_\epsilon^-|) + 1/3E(|e_\epsilon^+e_\theta^+|)$$

where θ and ϵ refers to components of the irreducible representation e.

We apply now this method to the calculation of the MLCT multiplet structure of the title compound. The relevant frontier orbitals involved in the MLCT states are depicted in Figure 1. The ground state is $(d\pi{:}e)^4$ $(d\pi{:}a_1)^2$ $^1A_1$. When all singly excited states within this manifold are considered, our procedure yields the following nonredundant determinantal excitations to be calculated in an individual DF calculation according to the method described in section 2.1:

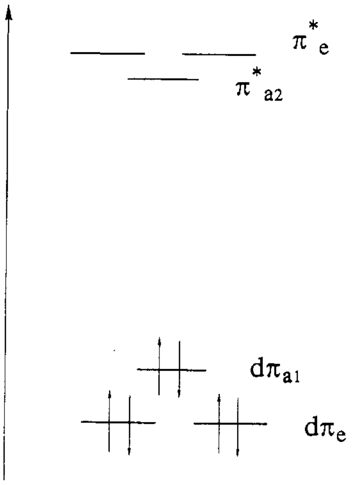

Figure 1. Frontier orbitals of $[Ru(bpy)_3]^{2+}$.

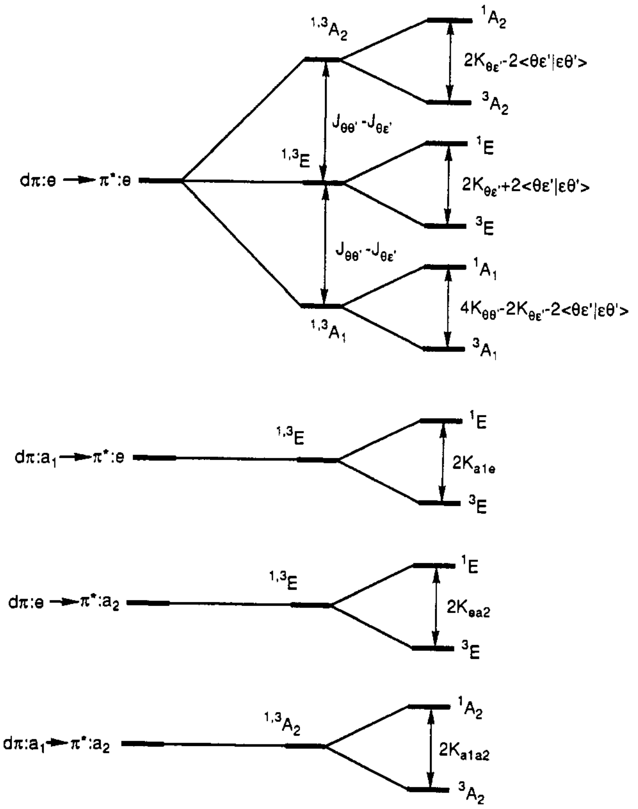

Figure 2. MLCT states of $[Ru(bpy)_3]^{2+}$.

ε_1 = excitation energy of $(d\pi{:}a_1)\alpha\rightarrow(\pi^*{:}a_2)\alpha$
ε_2 = excitation energy of $(d\pi{:}e\text{-}1)\alpha\rightarrow(\pi^*{:}a_2)\beta$
ε_3 = excitation energy of $(d\pi{:}a_1)\alpha\rightarrow(\pi^*{:}a_2)\beta$
ε_5 = excitation energy of $(d\pi{:}e\text{-}1)\alpha\rightarrow(\pi^*{:}e\text{-}2)\alpha$
ε_6 = excitation energy of $(d\pi{:}e\text{-}1)\alpha\rightarrow(\pi^*{:}e\text{-}1)\beta$
ε_7 = excitation energy of $(d\pi{:}a_1)\alpha\rightarrow(\pi^*{:}e\text{-}1)\alpha$
ε_8 = excitation energy of $(d\pi{:}e\text{-}1)\alpha\rightarrow(\pi^*{:}a_2)\alpha$
ε_9 = excitation energy of $(d\pi{:}e\text{-}1)\alpha\rightarrow(\pi^*{:}e\text{-}2)\beta$
ε_{10} = excitation energy of $(d\pi{:}e\text{-}1)\alpha\rightarrow(\pi^*{:}e\text{-}1)\alpha$
ε_{11} = excitation energy of $(d\pi{:}a_1)\alpha\rightarrow(\pi^*{:}e\text{-}1)\beta$

The relation between these excitation energies and the first-order state

---

[28] Daul, C. *J. Chim. Phys.* **1989**, *86*, 703.

Table 1. First-Order Multiplet Energies Expressed in Terms of Determinantal Excitation Energies and Two-Electron Electrostatic Integrals

state	single determinant energy	energy (electrostatic 2-electron integrals)[a]
$(\mathrm{d}\pi:\mathrm{a}_1) \rightarrow (\pi^*:\mathrm{a}_2)\ {}^1\mathrm{A}_2$	$2\epsilon_1 - \epsilon_3$	$\Delta\epsilon - J_{\mathrm{a1a1}} + J_{\mathrm{a1a2}} + K_{\mathrm{a1a2}}$
$(\mathrm{d}\pi:\mathrm{a}_1) \rightarrow (\pi^*:\mathrm{a}_2)\ {}^3\mathrm{A}_2$	ϵ_3	$\Delta\epsilon - J_{\mathrm{a1a1}} + J_{\mathrm{a1a2}} - K_{\mathrm{a1a2}}$
$(\mathrm{d}\pi:\mathrm{a}_1) \rightarrow (\pi^*:\mathrm{e})\ {}^1\mathrm{E}$	$2\epsilon_7 - \epsilon_{11}$	$\Delta\epsilon - J_{\mathrm{a1a1}} + J_{\mathrm{a1e}} + K_{\mathrm{a1e}}$
$(\mathrm{d}\pi:\mathrm{a}_1) \rightarrow (\pi^*:\mathrm{e})\ {}^3\mathrm{E}$	ϵ_{11}	$\Delta\epsilon - J_{\mathrm{a1a1}} + J_{\mathrm{a1e}} - K_{\mathrm{a1e}}$
$(\mathrm{d}\pi:\mathrm{e}) \rightarrow (\pi^*:\mathrm{a}_2)\ {}^1\mathrm{E}$	$2\epsilon_8 - \epsilon_2$	$\Delta\epsilon + 3J_{\mathrm{ea2}} - 0.5J_{\theta\theta} - 2.5J_{\theta\epsilon}$
$(\mathrm{d}\pi:\mathrm{e}) \rightarrow (\pi^*:\mathrm{a}_2)\ {}^3\mathrm{E}$	ϵ_2	$\Delta\epsilon + 3J_{\mathrm{ea2}} - 0.5J_{\theta\mathrm{J}} - 2.5J_{0\epsilon} - 2K_{\mathrm{ea2}}$
$(\mathrm{d}\pi:\mathrm{e}) \rightarrow (\pi^*:\mathrm{e})\ {}^1\mathrm{A}_1$	$(-4\epsilon_5 - 11\epsilon_6 + \epsilon_9 + 20\epsilon_{10})/6$	$\Delta\epsilon - 0.5J_{\theta\mathrm{J}} - 2.5J_{\theta\epsilon} - 0.5J_{\theta\theta'} + 2.5J_{\theta\epsilon\mu} + 3K_{\theta\theta'} - 3K_{\theta\epsilon'} - 2\langle\theta\epsilon'\|\epsilon\theta'\rangle$
$(\mathrm{d}\pi:\mathrm{e}) \rightarrow (\pi^*:\mathrm{e})\ {}^3\mathrm{A}_1$	$1.5\epsilon_6 - 0.5\epsilon_9$	$\Delta\epsilon - 0.5J_{\theta\mathrm{J}} - 2.5J_{\theta\epsilon} + 0.5J_{\theta\theta'} + 2.5J_{\theta\epsilon'} - K_{\theta\theta'} - K_{\theta\epsilon'}$
$(\mathrm{d}\pi:\mathrm{e}) \rightarrow (\pi^*:\mathrm{e})\ {}^1\mathrm{A}_2$	$(20\epsilon_5 + \epsilon_6 - 11\epsilon_9 - 4\epsilon_{10})/6$	$\Delta\epsilon - 0.5J_{\theta\theta} - 2.5J_{\theta\epsilon} + 2.5J_{\theta\theta'} + 0.5J_{\theta\epsilon'} - K_{\theta\theta'} + K_{\theta\epsilon'} - 2\langle\theta\epsilon'\|\epsilon\theta'\rangle$
$(\mathrm{d}\pi:\mathrm{e}) \rightarrow (\pi^*:\mathrm{e})\ {}^3\mathrm{A}_2$	$-0.5\epsilon_6 + 1.5\epsilon_9$	$\Delta\epsilon - 0.5J_{\theta\mathrm{J}} - 2.5J_{\theta\epsilon} + 2.5J_{\theta\theta'} + 0.5J_{\theta\epsilon'} - K_{\theta\theta'} - K_{\theta\epsilon'}$
$(\mathrm{d}\pi:\mathrm{e}) \rightarrow (\pi^*:\mathrm{e})\ {}^1\mathrm{E}$	$(4\epsilon_5 - \epsilon_6 - \epsilon_9 + 4\epsilon_{10})/6$	$\Delta\epsilon - 0.5J_{\theta\theta} - 2.5J_{\theta\epsilon} + 1.5J_{\theta\theta'} + 1.5J_{\theta\epsilon'} - K_{\theta\theta'} + K_{\theta\epsilon'} - 2\langle\theta\epsilon'\|\epsilon\theta'\rangle$
$(\mathrm{d}\pi:\mathrm{e}) \rightarrow (\pi^*:\mathrm{e})\ {}^3\mathrm{E}$	$0.5\epsilon_6 + 0.5\epsilon_9$	$\Delta\epsilon - 0.5J_{\theta\theta} - 2.5J_{\theta\epsilon} + 1.5J_{\theta\theta'} + 1.5J_{\theta\epsilon'} - K_{\theta\theta'} - K_{\theta\epsilon'}$

[a] Where $\Delta\epsilon$ refers to the separation of the corresponding MO energies; J and K refer respectively to Coulomb and exchange integrals; θ and ϵ denote the two components of $(\mathrm{d}\pi:\mathrm{e})$, whereas θ' and ϵ' refer to the two components of $(\pi^*:\mathrm{e})$, respectively.

energies is given in Table 1. This table gives also the relation between the state energies and the corresponding Coulomb and exchange integrals. The same result is also shown in a more pictorial fashion in Figure 2. In this latter representation the horizontal bars on the left-hand side of the figure represent the configurational barycenters, the bars in the middle represent the differences in Coulomb interaction between the different states, and finally the bars on the right-hand side show the result of exchange interaction.

A comparison of these formulae with the treatment of the electrostatic interaction by Kober–Meyer[15a] and by Ferguson–Herren[15b] shows that in the two latter models the difference of the Coulomb integrals $J_{\mathrm{aa}} - J_{\mathrm{ab}}$ is always neglected and that the exchange integrals K_{ab} for the different excited configurations are approximated by one single averaged parameter K_{av}.

For the sake of completeness, the off-diagonal matrix elements (CI matrix) expressed in terms of electrostatic two-electron matrix elements, which are neither of Coulomb type nor of exchange type, are given in Tables 2a–d.

2.3 Spin–Orbit Coupling. The inclusion of spin–orbit coupling in this calculation is important because of the large spin–orbit coupling constant of Ru ($\zeta_{4\mathrm{d}} \approx 1000$ cm^{-1}).[15] Due to this interaction the electrostatic multiplets obtained so far are further split into spin–orbit components. Their classification according to the double group D_3^* yields:

$$^1\mathrm{A}_1 \rightarrow \mathrm{A}_1$$

$$^3\mathrm{A}_1 \rightarrow \mathrm{A}_2 + \mathrm{E}$$

$$^1\mathrm{A}_2 \rightarrow \mathrm{A}_2$$

$$^3\mathrm{A}_2 \rightarrow \mathrm{A}_1 + \mathrm{E}$$

$$^1\mathrm{E} \rightarrow \mathrm{E}$$

$$^3\mathrm{E} \rightarrow \mathrm{A}_1 + \mathrm{A}_2 + 2\mathrm{E}$$

The calculation of the interaction matrix $\langle\psi_i|\mathrm{SO}|\psi_j\rangle$ is easily obtained from the multiplet wave function in eq 2 as

$$\langle\psi_i|\mathrm{SO}|\psi_j\rangle = \sum_{\mu,\nu} c_{i\mu}c_{i\nu}\langle\phi_\mu|\mathrm{SO}|\phi_\nu\rangle \tag{8}$$

The evaluation of these latter elements gives (χ_k refers to a spin–orbital)

$$\langle\phi_\mu|\mathrm{SO}|\phi_\mu\rangle = \sum_k \langle\chi_k|\mathrm{SO}|\chi_k\rangle \tag{9a}$$

in case both determinants are equal,

$$\langle\phi_\mu|\mathrm{SO}|\phi_\nu\rangle = \langle\chi_k|\mathrm{SO}|\chi_l\rangle \tag{9b}$$

in case the two determinants differ in exactly one spin–orbital (i.e. χ_k and χ_l refer to these spin–orbitals), and

$$\langle\phi_\mu|\mathrm{SO}|\phi_\nu\rangle = 0 \tag{9c}$$

otherwise. Finally the one-electron spin–orbit coupling matrix elements $\langle\chi_k|\mathrm{SO}|\chi_l\rangle$ are evaluated according to the method outlined in ref 27. The result of this calculation is presented in Table 3. In this table C_γ (γ = e, a$_1$, e′) denotes the MO coefficient of the Ru 4d atomic orbital; e refers to dπ:e, a$_1$ to dπ:a$_1$, and e′ to π^*:e orbitals.

A comparison of the formulae in Table 3 with the treatment of the spin–orbit coupling by Kober–Meyer[15a] and by Ferguson–Herren[15b] shows that in the two latter models the delocalization of the 4dπ electrons into the π^* orbitals of bpy is completely neglected.

Table 2. Off-Diagonal (2nd-Order Contribution) Electrostatic Matrix Elements

(a) Matrix Elements for ^{1}E

$(\mathrm{d}\pi:\mathrm{a}_1) \rightarrow (\pi^*:\mathrm{e})$	cf. Table 1		
$(\mathrm{d}\pi:\mathrm{e}) \rightarrow (\pi^*:\mathrm{a}_2)$	$2\langle \mathrm{a}_1\epsilon'\|\mathrm{a}_2\theta\rangle + \langle \mathrm{a}_2\theta'\|\mathrm{a}_1\epsilon\rangle$	cf. Table 1	
$(\mathrm{d}\pi:\mathrm{e}) \rightarrow (\pi^*:\mathrm{e})$	$2\sqrt{2}\langle\theta'\epsilon\|\mathrm{a}_1\theta'\rangle - \sqrt{2}\langle\theta'\theta'\|\mathrm{a}_1\theta\rangle$	$\sqrt{2}\langle \mathrm{a}_2\mathrm{a}_2\|\theta\theta'\rangle - \langle \mathrm{a}_2\theta\|\mathrm{a}_2\theta'\rangle$	cf. Table 1
	$(\mathrm{d}\pi:\mathrm{a}_1) \rightarrow (\pi^*:\mathrm{e})$	$(\mathrm{d}\pi:\mathrm{e}) \rightarrow (\pi^*:\mathrm{a}_2)$	$(\mathrm{d}\pi:\mathrm{e}) \rightarrow (\pi^*:\mathrm{e})$

(b) Matrix Elements for ^{3}E

$(\mathrm{d}\pi:\mathrm{a}_1) \rightarrow (\pi^*:\mathrm{e})$	cf. Table 1		
$(\mathrm{d}\pi:\mathrm{e}) \rightarrow (\pi^*:\mathrm{a}_2)$	$\langle \mathrm{a}_2\theta'\|\mathrm{a}_1\epsilon\rangle$	cf. Table 1	
$(\mathrm{d}\pi:\mathrm{e}) \rightarrow (\pi^*:\mathrm{e})$	$-\sqrt{2}\langle\theta'\theta'\|\mathrm{a}_1\theta\rangle$	$-\langle \mathrm{a}_2\theta\|\mathrm{a}_2\theta'\rangle$	cf. Table 1
	$(\mathrm{d}\pi:\mathrm{a}_1) \rightarrow (\pi^*:\mathrm{e})$	$(\mathrm{d}\pi:\mathrm{e}) \rightarrow (\pi^*:\mathrm{a}_2)$	$(\mathrm{d}\pi:\mathrm{e}) \rightarrow (\pi^*:\mathrm{e})$

(c) Matrix Elements for ^{1}A$_2$

$(\mathrm{d}\pi:\mathrm{a}_1) \rightarrow (\pi^*:\mathrm{a}_2)$	cf. Table 1	
$(\mathrm{d}\pi:\mathrm{e}) \rightarrow (\pi^*:\mathrm{e})$	$2\sqrt{2}\langle\theta'\epsilon\|\mathrm{a}_1\mathrm{a}_2\rangle - \sqrt{2}\langle \mathrm{a}_2\theta'\|\mathrm{a}_1\epsilon\rangle$	cf. Table 1
	$(\mathrm{d}\pi:\mathrm{a}_1) \rightarrow (\pi^*:\mathrm{a}_2)$	$(\mathrm{d}\pi:\mathrm{e}) \rightarrow (\pi^*:\mathrm{e})$

(d) Matrix Elements for ^{3}A$_2$

$(\mathrm{d}\pi:\mathrm{a}_1) \rightarrow (\pi^*:\mathrm{a}_2)$	cf. Table 1	
$(\mathrm{d}\pi:\mathrm{e}) \rightarrow (\pi^*:\mathrm{e})$	$-\sqrt{2}\langle \mathrm{a}_2\theta'\|\mathrm{a}_1\epsilon\rangle$	cf. Table 1
	$(\mathrm{d}\pi:\mathrm{a}_1) \rightarrow (\pi^*:\mathrm{a}_2)$	$(\mathrm{d}\pi:\mathrm{e}) \rightarrow (\pi^*:\mathrm{e})$

3. Results and Discussion

The MO diagram of $[\mathrm{Ru(bpy)_3}]^{2+}$ is well-known from previous electronic structure calculations.[15–19] The relevant molecular orbitals involved in the major photophysical and photochemical properties are well characterized. The composition and energies of these MO's, for the present study, are given in Table 4. From inspection of this table it is seen that the two highest occupied molecular orbitals dπ:e and dπ:a$_1$ have, as expected, predominant metal character. In fact they correspond to the t$_{2g}$ subshell in O_h symmetry and are π antibonding. The first one with e symmetry is a combination of 4dπ(Ru) with π orbitals of bpy that are antisymmetric (irreducible representation b$_2$) upon rotation about the C_2 axis of bpy. The second one has a$_1$ symmetry and is a combination of 4dπ(Ru) with π orbitals of bpy that are symmetric (irreducible representation a$_2$) upon rotation about

Table 3. Spin–Orbit Coupling Matrix among the Frontier Spin Orbitals[a]

spin–orbit coupling	$\|(d\pi{:}a_1)\alpha\rangle$	$\|(d\pi{:}a_1)\beta\rangle$	$\|(d\pi{:}\epsilon\text{-}1)\alpha\rangle$	$\|(d\pi{:}e\text{-}1)\beta\rangle$	$\|(d\pi{:}e)\alpha\rangle$
$\langle(d\pi{:}a_1)\alpha\|$	0	0	0	$C_{a1}C_e(-1+i)\zeta/\sqrt{8}$	$C_{a1}C_e i\zeta/\sqrt{6}$
$\langle(d\pi{:}a_1)\alpha\|$	0	0	$C_{a1}C_e(1+i)\zeta/\sqrt{8}$	0	$C_{a1}C_e(1-i)\zeta/\sqrt{24}$
$\langle(d\pi{:}e\text{-}1)\alpha\|$	0	$C_{a1}C_e(1-i)\zeta/\sqrt{8}$	0	0	$-C_eC_e i\zeta/\sqrt{12}$
$\langle(d\pi{:}e\text{-}1)\beta\|$	$-C_{a1}C_e(1+i)\zeta\sqrt{8}$	0	0	0	$C_eC_e(1\text{-}i)\zeta/\sqrt{12}$
$\langle(d\pi{:}e\text{-}2)\alpha\|$	$-C_{a1}C_e i\zeta/\sqrt{6}$	$C_{a1}C_e(1+\mathrm{i})\zeta/\sqrt{24}$	$C_eC_e i\zeta/\sqrt{12}$	$C_eC_e(1+i)\zeta/\mathrm{sqr}12$	0
$\langle(d\pi{:}e\text{-}2)\beta\|$	$C_{a1}C_e(-1+i)\zeta/\sqrt{24}$	$C_{a1}/C_e i\zeta/\sqrt{6}$	$C_eC_e(-1+i)\zeta/\sqrt{12}$	$-C_eC_e i\zeta/\sqrt{12}$	0
$\langle(\pi^*{:}e\text{-}1)\alpha\|$	$-C_{a1}C_{e'} i\zeta/\sqrt{3}$	$C_{a1}C_{e'}(1+i)\zeta/\sqrt{12}$	$-C_eC_{e'} i\zeta\sqrt{(2/3)}$	$-C_eC_{e'}(1+i)\zeta/\sqrt{24}$	0
$\langle(\pi^*{:}e\text{-}1)\beta\|$	$C_{a1}C_{e'}(-1+i)\zeta/\sqrt{12}$	$C_{a1}C_{e'} i\zeta/\sqrt{3}$	$C_eC_{e'}(1\text{-}i)\zeta/\sqrt{24}$	$C_eC_{e'} i\zeta\sqrt{(2/3)}$	$-C_eC_{e'}(1+i)\zeta/\sqrt{8}$
$\langle(\pi^*{:}e\text{-}2)\alpha\|$	0	$C_{a1}C_{e'}(-1+i)\zeta/2$	0	$C_eC_{e'}(1-i)\zeta/\sqrt{8}$	0
$\langle(\pi^*{:}e\text{-}2)\beta\|$	$C_{a1}C_{e'}(1+i)\zeta/2$	0	$-C_eC_{e'}(1+i)\zeta/\sqrt{8}$	0	$C_eC_{e'}(1-i)\zeta\sqrt{(3/8)}$

spin–orbit coupling	$\|(d\pi{:}e\text{-}1)\beta\rangle$	$\|(\pi^*{:}e\text{-}1)\alpha\rangle$	$\|(\pi^*{:}e\text{-}1)\beta\rangle$	$\|(\pi^*{:}e\text{-}2)\alpha\rangle$	$\|(\pi^*{:}e\text{-}2)\beta\rangle$
$\langle(d\pi{:}a_1)\alpha\|$	$-C_{a1}C_e(1+i)\zeta/\sqrt{24}$	$C_{a1}C_{e'} i\zeta/\sqrt{3}$	$-C_{a1}C_{e'}(1+i)\zeta/\sqrt{12}$	0	$C_{a1}C_{e'}(1-i)\zeta/2$
$\langle(d\pi{:}a_1)\alpha\|$	$-C_{a1}C_e i\zeta/\sqrt{6}$	$C_{a1}C_{e'}(1-i)\zeta/\sqrt{12}$	$-C_{a1}C_{e'} i\zeta/\sqrt{3}$	$-C_{a1}C_{e'}(1+i)\zeta/2$	0
$\langle(d\pi{:}e\text{-}1)\alpha\|$	$-C_eC_e(1+i)\zeta/\sqrt{12}$	$C_eC_{e'} i\zeta\sqrt{(2/3)}$	$C_eC_{e'}(1+i)\zeta/\sqrt{24}$	0	$C_eC_{e'}(-1+i)\zeta/\sqrt{8}$
$\langle(d\pi{:}e\text{-}1)\beta\|$	$C_eC_e i\zeta/\sqrt{12}$	$C_eC_{e'}(-1+i)\zeta/\sqrt{24}$	$-C_eC_{e'} i\zeta\sqrt{(2/3)}$	$C_eC_{e'}(1+i)\zeta/\sqrt{8}$	0
$\langle(d\pi{:}e\text{-}2)\alpha\|$	0	0	$C_eC_{e'}(-1+i)\zeta/\sqrt{8}$	0	$C_eC_{e'}(1+i)\zeta\sqrt{(3/8)}$
$\langle d\pi{:}e\text{-}2)\beta\|$	0	$C_eC_{e'}(1+i)\zeta/\sqrt{8}$	0	$C_eC_{e'}(-1+i)\zeta\sqrt{(3/8)}$	0
$\langle(\pi^*{:}e\text{-}1)\alpha\|$	$C_eC_{e'}(1-i)\zeta/\sqrt{8}$	0	0	0	0
$\langle(\pi^*{:}e\text{-}2)\alpha\|$	$-C_eC_{e'}(1+i)\zeta\sqrt{(3/8)}$	0	0	0	0
$\langle(\pi^*{:}e\text{-}2)\beta\|$	0	0	0	0	0

[a] π^*:a2 is omitted in this table, since spin–orbit coupling of this orbital vanishes with all the other orbitals of the basis set.

Table 4. Composition and Energies of the Frontier MO's of $[Ru(bpy)_3]^{2+}$

composition[a]	orbital	energy (eV)
87.8% $\pi^*_4(b_2)$ + 9.5% Ru(4d)	π^*:e	−8.869
93.4% $\pi^*_4(b_2)$ + 3.4% $\pi^*_5(b_2)$ + 1.2% $\pi_3(b_2)$	π^*:a_2	−9.038
83.3% Ru(4d) + 8.5% $\pi_1(a_2)$ + 3.4% $\pi_3(a_2)$	dπ:a_1	−10.978
72.7% Ru(4d) + 8.4% $\pi_3(b_2)$ + 6.1% $\pi^*_4(b_2)$ + 3.4% $\pi^*_5(b_2)$ + 2.5% $\pi_2(b_2)$	dπ:e	−11.303

[a] π_i and π^*_i refer to respectively an occupied and empty π-orbital of bpy; the symbols a_2 and b_2 denote the irreducible representation of these π-orbitals in C_{2v} symmetry.

the C_2 axis of bpy. On the other hand, the two lowest unoccupied molecular orbitals, π^*:a_2 and π^*:e, are almost equivalent to a combination of the lowest π^* orbital of the three bpy ligands. This latter one is antisymmetric (irreducible representation b_2) upon rotation about the C_2 axis of bpy. The LUMO with a_2 symmetry is purely a ligand type. The second unoccupied molecular orbital with e symmetry has also some metal character.

After obtaining a self-consistent solution to the ground state, we turn to the calculation of the unrestricted excited configurations as described in section 2.1. The results of these calculations are displayed in Table 5. Inspection of this table shows that the single determinantal energies of the determinants needed for the calculation of all MLCT first-order state energies are thus obtained. Using the expressions in Table 1 yields these energies as shown in Table 6. The results in this table do not yet include spin–oribit coupling. However, the comparison of these results with Figure 2 is interesting. It is thus possible to obtain numerical values for all exchange integrals and for some Coulomb integrals. The result of such a calculation is shown in Table 7. The values thus obtained are quite reasonable. In particular it is seen that the exchange integral $K_{\theta\theta'}$ between the first component of dπ:e and the first component of π^*:e has by far the largest value.

The final step in our calculation of the MLCT states of $[Ru(bpy)_3]^{2+}$ is the calculation of their spin–orbit splitting. This is done by calculating the complete, 36 × 36, interaction matrix and by solving it; 36 is the total number of MLCT components. This interaction matrix is readily obtained according to the method outlined in section 2.3 and by adding the values obtained in Table 6 to the diagonal. Thus, the electrostatic interaction acts in first order and the spin–orbit coupling in second order. The second-order electrostatic interaction (cf. Table 4) is neglected in the present calculation since we believe that this latter interaction is at least 1 order of magnitude smaller than the spin–orbit coupling. This statement is based on the fact that off-diagonal matrix elements corresponding to this interaction depend upon two-electron electrostatic integrals which are neither of Coulomb type

Table 5. Determinantal Excitation Energies of $[Ru(bpy)_3]^{2+}$

type of excitation[a]	ΔE: restricted config – ground state	ΔE: spin-unrestricted "determinant" – restricted config	excitation energy (eV)
$(d\pi{:}a_1)\alpha \rightarrow (\pi^*{:}a_2)\alpha$	2.705	−0.190[b]	2.515 ($=\epsilon_1$)
$(d\pi{:}a_1)\alpha \rightarrow (\pi^*{:}a_2)\beta$	2.705	−0.215[c]	2.490 ($=\epsilon_3$)
$(d\pi{:}a_1)\alpha \rightarrow (\pi^*{:}e\text{-}1)\alpha$	2.793	+0.046	2.839 ($=\epsilon_7$)
$(d\pi{:}a_1)\alpha \rightarrow (\pi^*{:}e\text{-}1)\beta$	2.793	+0.006	2.799 ($=\epsilon_{11}$)
$(d\pi{:}e\text{-}1)\alpha \rightarrow (\pi^*{:}a_2)\alpha$	2.751	−0.060	2.691 ($=\epsilon_8$)
$(d\pi{:}e\text{-}1)\alpha \rightarrow (\pi^*{:}a_2)\beta$	2.751	−0.079	2.672 ($=\epsilon_2$)
$(d\pi{:}e\text{-}1)\alpha \rightarrow (\pi^*{:}e\text{-}1)\alpha$	2.835	+0.118	2.953 ($=\epsilon_{10}$)
$(d\pi{:}e\text{-}1)\alpha \rightarrow (\pi^*{:}e\text{-}1)\beta$	2.835	+0.091	2.876 ($=\epsilon_6$)
$(d\pi{:}e\text{-}1)\alpha \rightarrow (\pi^*{:}e\text{-}2)\alpha$	2.835	+0.266	3.101 ($=\epsilon_5$)
$(d\pi{:}e\text{-}1)\ \alpha \rightarrow (\pi^*{:}e\text{-}2)\beta$	2.835	+0.233	3.068 ($=\epsilon_9$)

[a] e-1 and e-2 refer to the first and to the second component of the irreducible representation e, respectively; α and β denote the up and down spin component respectively. [b] If the SCF procedure for this unrestricted excited configuration is carried out until convergence is reached, ΔE(converged) = 0.212, which differs unsignificantly from the reported value obtained after one SCF cycle. [c] Same as above; ΔE(converged) = 0.231.

Table 6. Energies of the MLCT States without Spin–Orbit Coupling

excited config	state	energy (10^3 cm^{-1})	excited config	state	energy (10^3 cm^{-1})
$d\pi_{a1} \rightarrow \pi^*_{a2}$	$^3A_2$	20.08	$d\pi_{a1} \rightarrow \pi^*_e$	^1E	23.22
$d\pi_{a1} \rightarrow \pi^*_{a2}$	$^1A_2$	20.49	$d\pi_e \rightarrow \pi^*_e$	^3E	23.97
$d\pi_e \rightarrow \pi^*_{a2}$	^3E	21.56	$d\pi_e \rightarrow \pi^*_e$	$^1A_1$	24.32
$d\pi_e \rightarrow \pi^*_{a2}$	^1E	21.86	$d\pi_e \rightarrow \pi^*_e$	^1E	24.56
$d\pi_e \rightarrow \pi^*_e$	$^3A_1$	22.42	$d\pi_e \rightarrow \pi^*_e$	$^3A_2$	25.52
$d\pi_{a1} \rightarrow \pi^*_e$	^3E	22.58	$d\pi_e \rightarrow \pi^*_e$	$^1A_2$	26.00

Table 7. Electrostatic Two-Electron Integrals

two-electron integral[a]	value (cm^{-1})	two-electron integral[a]	value (cm^{-1})
$J_{\theta\theta'} - J_{\theta\epsilon'}$	1549	$K_{\theta\theta'}$	621.3
K_{a1a2}	202	$K_{\theta\epsilon'}$	266.3
K_{a1e}	322.5	$\langle\theta\epsilon'\|\epsilon\theta'\rangle$	29.8
K_{ea2}	153.5		

[a] Cf. with Table 1 for the notation.

Table 8. Energies of the MLCT States Including Spin–Orbit Coupling

composition[a]	state	predicted energy (10^3 cm^{-1})	obsd energy[29,30] (10^3 cm^{-1})
$85\%\ {}^3A_2(d\pi_{a1} \rightarrow \pi^*_{a2}) + 14\%\ {}^3E(d\pi_e \rightarrow \pi^*_{a2})$	A_1	19.877	
$87\%\ {}^3A_2(d\pi_{a1} \rightarrow \pi^*_{a2}) + 7\%\ {}^3E(d\pi_e \rightarrow \pi^*_{a2})$	E	19.896	18.47
$77\%\ {}^1A_2(d\pi_{a1} \rightarrow \pi^*_{a2}) + 22\%\ {}^3E(d\pi_e \rightarrow \pi^*_{a2})$	A_2	20.213	18.95
$85\%\ {}^3E(d\pi_e \rightarrow \pi^*_{a2}) + 14\%\ {}^3A_2(d\pi_{a1} \rightarrow \pi^*_{a2})$	A_1	21.439	
$77\%\ {}^3E(d\pi_e \rightarrow \pi^*_{a2}) + 22\%\ {}^1A_2(d\pi_{a1} \rightarrow \pi^*_{a2})$	A_2	21.513	20.45
$66\%\ {}^3E(d\pi_e \rightarrow \pi^*_{a2}) + 21\%\ {}^1E(d\pi_e \rightarrow \pi^*_{a2})$	E	21.534	
$99\%\ {}^3E(d\pi_e \rightarrow \pi^*_{a2})$	E	21.938	
$57\%\ {}^3A_1(d\pi_e \rightarrow \pi^*_e) + 40\%\ {}^3E(d\pi_{a1} \rightarrow \pi^*_e)$	A_2	22.056	
$60\%\ {}^3A_1(d\pi_e \rightarrow \pi^*_e) + 34\%\ {}^3E(d\pi_{aq} \rightarrow \pi^*_e)$	E	22.103	
$72\%\ {}^1E(d\pi_e \rightarrow \pi^*_{a2}) + 27\%\ {}^3E(d\pi_e \rightarrow \pi^*_{a2})$	E	22.125	21.5 (strong)
$88\%\ {}^3E(d\pi_{aq} \rightarrow \pi^*_e) + 8\%\ {}^3E(d\pi_e \rightarrow \pi^*_e)$	E	22.399	
$92\%\ {}^3E(d\pi_{a1} \rightarrow \pi^*_e) + 5\%\ {}^1A_1(d\pi_e \rightarrow \pi^*_e)$	A_1	22.450	
$46\%\ {}^3E(d\pi_{a1} \rightarrow \pi^*_e) + 20\%\ {}^3A_1(d\pi_e \rightarrow \pi^*_e)$	E	22.566	
$58\%\ {}^3E(d\pi_{a1} \rightarrow \pi^*_e) + 41\%\ {}^3A_1(d\pi_e \rightarrow \pi^*_e)$	A_2	22.923	24.74
$56\%\ {}^1E(d\pi_{a1} \rightarrow \pi^*_e) + 19\%\ {}^3A_1(d\pi_e \rightarrow \pi^*_{a2})$	E	23.201	
$72\%\ {}^3E(d\pi_e \rightarrow \pi^*_e) + 22\%\ {}^1E(d\pi_{a1} \rightarrow \pi^*_e)$	E	23.948	
$78\%\ {}^3E(d\pi_e \rightarrow \pi^*_e) + 11\%\ {}^1E(d\pi_e \rightarrow \pi^*_e)$	E	24.000	
$99\%\ {}^3E(d\pi_e \rightarrow \pi^*_e)$	A_1	24.348	
$99\%\ {}^3E(d\pi_e \rightarrow \pi^*e)$	A_2	24.354	25.60
$89\%\ {}^1A_1(d\pi_e \rightarrow \pi^*_e) + 4\%\ {}^3A_2(d\pi_e \rightarrow \pi^*_e)$	A_1	24.362	
$85\%\ {}^1E(d\pi_e \rightarrow \pi^*_e) + 14\%\ {}^3E(d\pi_e \rightarrow \pi^*_e)$	E	24.766	23.3 (strong)
$97\%\ {}^3A_2(d\pi_e \rightarrow \pi^*_e) + 1\%\ {}^1E(d\pi_{a1} \rightarrow \pi^*_e)$	E	25.623	
$93\%\ {}^3A_2(d\pi_e \rightarrow \pi^*_e) + 5\%\ {}^1A_1(d\pi_e \rightarrow \pi^*_e)$	A_1	25.663	
$99\%\ {}^1A_2(d\pi_e \rightarrow \pi^*_e)$	A_2	26.089	26.13

[a] Only the major parent states are reported.

nor of exchange type, i.e. integrals which are comparable to the last integral in Table 7 ($\langle \theta\epsilon' | \epsilon\theta' \rangle = 29.8$ cm^{-1}). On the other hand the spin–orbit coupling constant for 4d(Ru) is 990 cm^{-1}. Thus, the neglect of second-order electrostatic interaction is justified in this case. Solving the secular equation associated with the 36 × 36 spin–orbit matrix yields the results reported in Table 8. In this table we have gathered together the major results of our calculation with the spectroscopic data obtained from single-crystal polarization work[29] and MCD.[30]

Bearing in mind that this calculation does not include any adjustable parameter, the comparison of these results with unambiguously assigned transition energies from ref 29 shows an acceptable agreement. Beyond this overall agreement, the main interest for the title compound is the identification of the luminescent states. Inspection of Table 8 shows clearly that, according to this calculation, the lowest excited state is $(d\pi{:}a_1) \rightarrow (\pi^*{:}a_2)\ {}^3A_2$ which splits by second-order spin–orbit coupling into an A_1 and an E component, the former lying 19 cm^{-1} below the latter one. Above the $^3A_2$ we find $(d\pi{:}a_1) \rightarrow (\pi^*{:}a_2)\ {}^1A_2$ (spin–orbit component: A_2) which belongs to the same excitation $(d\pi{:}a_1 \rightarrow \pi^*{:}a_2)$ and is separated from the lowest excited state by 356 cm^{-1}. These three levels are clearly isolated from all the other excited states by roughly 1500 cm^{-1}. We wish to emphasize once more that the figures given above are not accurate to 1 cm^{-1}. Comparison between predicted and observed data clearly indicates this. Despite this fact, a qualitative interpretation of these results yields some useful indications which can be used as a basis for a refined model.

4. Conclusion

The results obtained in this work demonstrate once more the good ability of DFT calculations to predict the energies of excited (MLCT) states with a reasonable accuracy of (1–2) × 10^3 cm^{-1}. This precision might not be enough to describe unambiguously the fine structure of the MLCT manifold of $[Ru(bpy)_3]^{2+}$. To solve this problem, a refined model is needed. Such a study, essentially based on a judicious parametrization of the electrostatic integrals in Table 1, is in progress. The results of this study will be published separately.

A further extension useful to this work would be the calculation of experimental quantities like e.g. *g*-values of the excited states and transition strengths. The evaluation of these properties could easily be undertaken within the same methodological frame in the near future.

Acknowledgment. This work is part of Project 20-29001.90 of the Swiss National Science Foundation.

---

(29) Felix, F.; Ferguson, J.; Güdel, H. U.; Ludi, A. *J. Am. Chem. Soc.* **1980**, *102*, 4096.

(30) Ferguson, J.; Krausz, E.; Vrbancich, J. *Chem. Phys. Lett.* **1986**, *131*, 463.